Investigating discrepancies between experimental solid-state NMR and GIPAW calculation: N=C-N ^{13}C and OH···O ^{1}H chemical shifts in pyridinium fumarates and their cocrystals

Emily K. Corlett[a], Helen Blade[b], Leslie P. Hughes[b], Philip J. Sidebottom[c], David Walker[a], Richard I. Walton[d] and Steven P. Brown[a*]

[a.] *Department of Physics, University of Warwick, Coventry, CV4 7AL*

[b.] *Pharmaceutical Development AstraZeneca, Macclesfield, SK10 2NA*

[c.] *Syngenta, Jealott's Hill International Research Centre, Bracknell, Berkshire, RG42 6EY*

[d.] *Department of Chemistry, University of Warwick, Coventry, CV4 7AL*

* S.P.Brown@warwick.ac.uk

Abstract

An NMR crystallography analysis is presented for four solid-state structures of pyridine fumarates and their cocrystals, using crystal structures deposited in the Cambridge Crystallographic Data Centre, CCDC. Experimental one-dimensional, one-pulse ^{1}H and ^{13}C cross-polarisation (CP) magic-angle spinning (MAS) nuclear magnetic resonance (NMR) and two-dimensional ^{14}N-^{1}H heteronuclear multiple-quantum coherence MAS NMR spectra are compared with gauge-including projector augmented wave (GIPAW) calculations of the ^{1}H and ^{13}C chemical shifts and the ^{14}N shifts that additionally depend on the quadrupolar interaction. Considering the high ppm (>10 ppm) ^{1}H resonances, while there is good agreement (within 0.4 ppm) between experiment and GIPAW calculation for the hydrogen-bonded NH moieties, the hydrogen-bonded fumaric acid OH resonances are 1.2 to 1.9 ppm higher in GIPAW calculation as compared to experiment. For the cocrystals of a salt and a salt formed by 2-amino-5-methylpyridinium and 2-amino-6-methylpyridinium ions, a large discrepancy of 4.2 and 5.9 ppm between experiment and GIPAW calculation is observed for the quaternary ring carbon ^{13}C resonance that is directly bonded to two nitrogens (in the ring and in the amino group). By comparison, there is excellent agreement (within 0.2 ppm) for the quaternary ring carbon ^{13}C resonance directly bonded to the ring nitrogen for the salt and cocrystal of a salt formed by 2,6-lutidinium and 2,5-lutidine, respectively.

Introduction

The NMR crystallography approach has been increasingly utilised to provide a detailed characterisation of solid systems, whereby solid-state magic-angle spinning (MAS) NMR and density functional theory (DFT) calculations, in particular using the gauge including projector augmented wave (GIPAW) method,[1] are used alongside complementary techniques such as X-ray diffraction (XRD).[2-6] The power of GIPAW has been demonstrated in numerous applications, notably providing a link between crystal

structures and NMR parameters, aiding both their development and validation[7-9] as well as adding further insight to investigations of intermolecular interactions.[10-15]

A key consideration is the level of agreement between experiment and calculation. For ^{1}H and ^{13}C solid-state NMR of organic molecules, there is a typical maximum discrepancy corresponding to ~1% of the chemical shift range, i.e., ~0.2 ppm and ~2 ppm for ^{1}H and ^{13}C, respectively.[16-20] Specifically, Engel et al have recently performed a Bayesian analysis and determined a discrepancy between experiment and GIPAW calculation of 2.9 ± 0.7 ppm for ^{13}C in organic molecular solids.[21] It is also known that the gradient of a plot of experimental versus calculated chemical shielding often deviates from unity, see for example reference.[22] For ^{13}C, this results in an undercalculation at low chemical shifts and an overcalculation at high chemical shifts, *e.g.* methyl and carboxylate carbons, respectively, when a single reference shielding is used for the entire spectrum. An alternative approach is to use different reference shieldings for different parts of the spectrum.[18]

Here we consider the four systems presented in Table 1. They are based on four differently substituted pyridine molecules and fumaric acid: specifically, two salts and two cocrystals of a salt are formed in the solid state. The structure of each system's asymmetric unit is given in Figure 1, alongside the atomic labels used throughout this work. Salt and cocrystal formation can alter the properties of a compound, such as stability, solubility and hygroscopicity, making them of considerable interest to pharmaceutical and agrochemical industries.[23-26] Salt formation in particular has been common practice in the development of active pharmaceutical ingredients for more than 25 years.[27] The observation of a salt or cocrystal form often depends on the position of a single proton,[9, 28] making NMR crystallography methods extremely useful for their characterisation. In this paper, we report the identification of a ^{1}H and a ^{13}C specific chemical environment within the systems listed in Table 1 (this Table states the CSD reference and number as well as the original literature reference for the crystal structure, and also the shorthand names used here) whose chemical shifts exhibit larger than expected discrepancies between experiment and GIPAW calculation.

Table 1: Solid-state structures available from the CCDC[29] investigated in this paper.

Name	Literature reference	CSD reference	CSD number
26L:F - 2,6-lutidinium hydrogen fumarate	Pan *et al.*[30]	MIBYEB	181445
25L:FFA - 2,5-lutidine hemi-fumarate fumaric acid	Haynes *et al.*[31]	RESGEC	615314
25AMP:FFA - 2-amino-5-methylpyridinium hemi-fumarate hemi-fumaric acid	Hemamalini *et al.*[32]	DUTNUC	788456
26AMP:F-H2 - 2-amino-6-methylpyridinium hemi-fumarate dihydrate	Selyani *et al.*[33]	COGCIN	1521964
FA - Fumaric acid	Brown[34]	FUMAAC	1161115

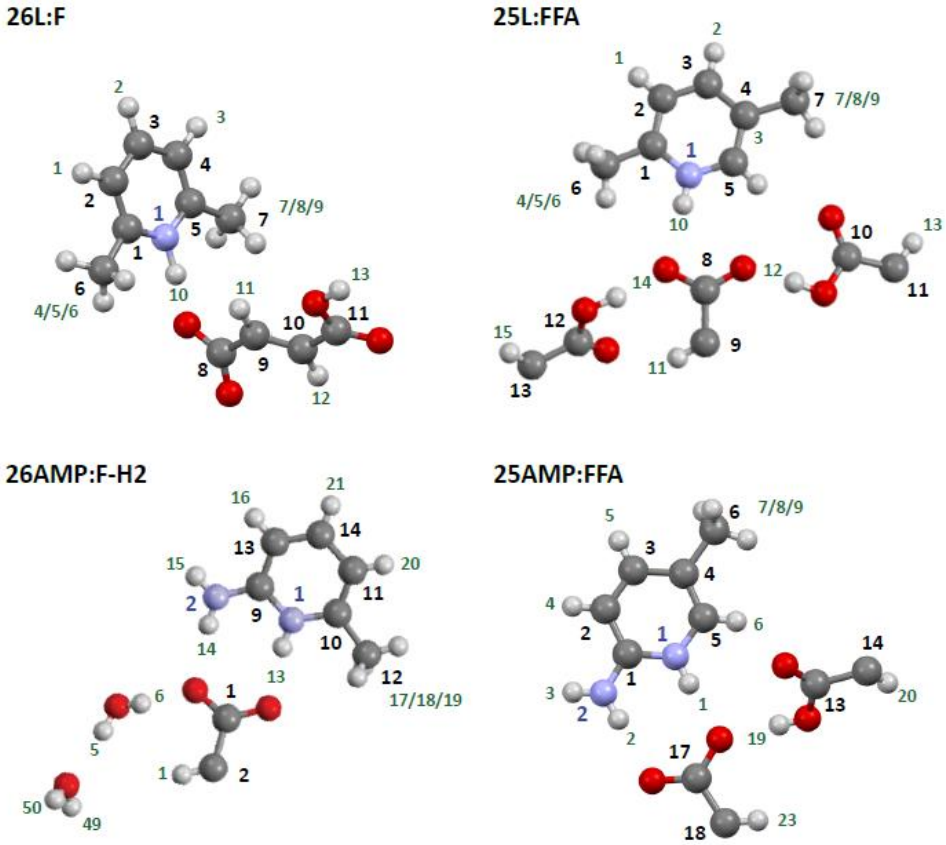

Figure 1: Asymmetric unit of 26L:F, 25L:FFA, 25AMP:FFA and 26AMP:F-H2 (clockwise from top left) with the atomic labels used in this work –black numbers, small green numbers and blue numbers correspond to labels for C, H and N, respectively. Nitrogen and Oxygen atoms are in blue and red, respectively.

Experimental

All chemicals were obtained from Sigma Aldrich (UK) at purities of 98% or higher and used without further purification. For each system, co-crystallisation was achieved by slow solvent evaporation over approximately 4 days. Powder XRD (see SI) was performed on a Panalytical X'Pert Pro MPD equipped

with a curved Ge Johansson monochromator, giving pure Cu $K_{\alpha 1}$ radiation, and a solid-state PiXcel detector. The powder samples were mounted on a zero-background offcut-Si holder, spinning at 30 rpm. Each sample was run with a step size of 0.013° and the time per step ranged from 750-3500 s, depending on the sample volume available.

Density functional theory (DFT) calculations were performed using CASTEP[35] Academic Release version 16.1. All calculations used the Perdew Burke Ernzerhof (PBE) exchange correlation functional,[36] a plane-wave basis set with ultrasoft pseudopotentials and a plane-wave cut-off energy of 700 eV. Integrals over the Brillouin zone were taken using a Monkhorst-Pack grid of minimum sample spacing $0.1 \times 2\pi$ $Å^{-1}$ (unless otherwise stated). The literature structures were downloaded from the Cambridge Crystallographic Data Centre (CCDC).[29] For all structures, geometry optimisation was performed with the unit cell parameters fixed. NMR parameters were calculated using the gauge-including projector-augmented wave (GIPAW)[1] method and were performed for the geometry optimised crystal structures.

The calculated isotropic chemical shifts (δ_{iso}^{calc}) were determined from the calculated chemical shieldings (σ_{calc}) by $\delta_{iso}^{calc} = \sigma_{ref} - \sigma_{calc}$, with calculated σ_{ref} values as stated in Table 2. σ_{ref} was determined for ^{1}H and ^{13}C by taking the sum of the average experimental chemical shift and the average GIPAW calculated absolute isotropic chemical shielding. This is equivalent to considering a plot of experimental versus calculated chemical shielding, where the (negative) gradient of the line of best fit is constrained to unity, for which the y-intercept of the line of best fit then corresponds to σ_{ref}.[37, 38]

Table 2: Reference shielding, σ_{ref}, for each system.

System	σ_{ref} (ppm)	
	^{1}H	^{13}C
26L:F	30.5	169.7
25L:FFA	29.9	169.5
25AMP:FFA	29.9	169.7
26AMP:F-H2	29.9	170.7
FA	30.0	-

Solid-state NMR experiments were performed on: (1) a Bruker Avance III spectrometer, operating at ^{1}H and ^{13}C Larmor frequencies of 500.0 MHz and 125.8 MHz, respectively; (2) a Bruker Avance II+ spectrometer, operating at ^{1}H, ^{13}C and ^{14}N Larmor frequencies of 600.0 MHz, 150.7 MHz and 43.4 MHz, respectively; (3) a Bruker Avance III HD spectrometer, operating at ^{1}H, ^{13}C and ^{14}N Larmor frequencies of 700.0 MHz, 176.0 MHz and 50.6 MHz, respectively.

1.3 mm HXY probes in double resonance mode were used for ^{1}H one-pulse MAS and 2D ^{14}N-^{1}H heteronuclear multiple-quantum correlation (HMQC)[39-42] (with R^3 recoupling[43, 44]) experiments, at a MAS frequency of 60 kHz. ^{1}H-^{13}C CP MAS were conducted at an MAS frequency of 12.5 kHz. Additional experimental details are stated in Table 3. The ^{1}H nutation frequency was 100 kHz (except during CP), corresponding to a ^{1}H 90° pulse duration of 2.5 μs. The 2D ^{14}N-^{1}H HMQC experiment employed a rotor-synchronised t_1 increment of 16.67 μs, 133 μs of R^3 recoupling and the States-TPPI method for sign discrimination.[45] For ^{1}H-^{13}C CP MAS experiments, SPINAL64[46] ^{1}H heteronuclear decoupling was applied during the acquisition of the ^{13}C FID, with a pulse duration of 5.9 μs at a nutation frequency of 100 kHz, and a 70 to 100% ramp[47] on the ^{1}H channel was used for the CP contact time with nutation frequencies of 47.5 and 60 kHz for ^{13}C and ^{1}H, respectively.

^{13}C and ^{1}H chemical shifts are referenced with respect to tetramethylsilane (TMS) via L-alanine at natural abundance as a secondary reference (1.1 ppm for the CH_3 ^{1}H resonance and 177.8 ppm for the CO ^{13}C resonance) corresponding to adamantane at 1.85 ppm (^{1}H)[48] and 38.5 ppm (^{13}C)[49]. ^{14}N shifts are referenced with respect to a saturated NH_4Cl aqueous solution via spectra of L-β-aspartyl-L-alanine at natural abundance (−284 ppm for the lower NH resonance at a Larmor frequency of 43.4 MHz) corresponding to liquid CH_3NO_2 at 0 ppm.[41, 50] The accuracy of determining ^{1}H, ^{13}C and ^{14}N shifts from MAS NMR spectra is estimated as ± 0.2, ± 0.1 and ± 5 ppm, respectively.

Table 3: Experimental MAS NMR parameters applied for each of the systems.

	^{1}H one-pulse			**^{14}N-^{1}H HMQC**				**^{1}H-^{13}C CP**				
	*	Co-added transients	Recycle delay (s)	*	Co-added transients	FIDs in t_1	Recycle delay (s)	*	Probe	Co-added transients	CP contact time (μs)	Recycle delay (s)
26L:F	**1**	16	100	**2**	16	240	60	**1**	4 mm HX	32	750	78
25L: FFA	**2**	8	10	**2**	16	192	15	**1**	4 mm HX	32	1500	60
25AMP :FFA	**3**	8	5	**2**	32	128	50	**2**	2.5 mm HX	64	2000	70
26AMP :F-H2	**2**	4	75	**3**	8	136	80	**2**	3.2 mm HX	32	1500	80

* Solid-state NMR experiments were performed at a ^{1}H Larmor frequency of: (1) 500.0 MHz, (2) 600.0 MHz, and (3) 700.0 MHz.

Results

We report here an NMR crystallography study of four related systems that are based on four differently substituted pyridine molecules and fumaric acid: specifically, two salts and two cocrystals of a salt. Their crystal structures have been previously reported and deposited in the CCDC as listed in Table 1 (note that the experimental and GIPAW calculated results for 26L:F have been previously presented in Ref. [15]). As noted above and expanded upon below, the focus of this paper is the identification of two specific chemical environments (see Fig. 2) for which there are significantly larger differences between their GIPAW calculated and experimental MAS NMR chemical shifts than expected. One discrepancy

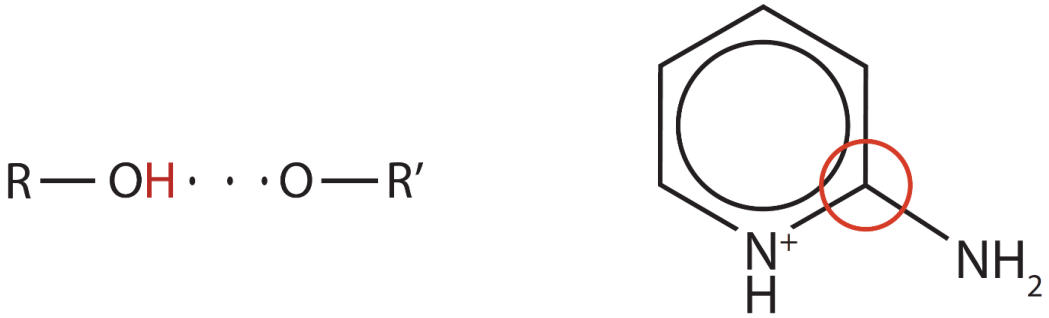

Figure 2: Chemical structures of the two environments which show large discrepancies between GIPAW calculated and experimental chemical shift: a ^{1}H in a OH···O hydrogen bond (left) and a quaternary ^{13}C between a pyridinium nitrogen and an amino nitrogen (right).

is for ^{1}H in a OH···O hydrogen bond and the other discrepancy is for a quaternary ^{13}C which is covalently bound to both a pyridinium nitrogen and an amino nitrogen.

^{1}H environment

Fig. 3 shows 1D ^{1}H one-pulse MAS spectra for each system containing an OH···O hydrogen bond, with stick spectra corresponding to GIPAW calculated chemical shifts for the geometry optimised crystal structures. Note that the experimental COOH ^{1}H chemical shift for fumaric acid (FA) is taken from the literature.[51] Assignments are made with the aid of both 2D ^{14}N-^{1}H HMQC MAS NMR spectra (Fig. 4) and GIPAW calculation (SI, Tables S1-S5).

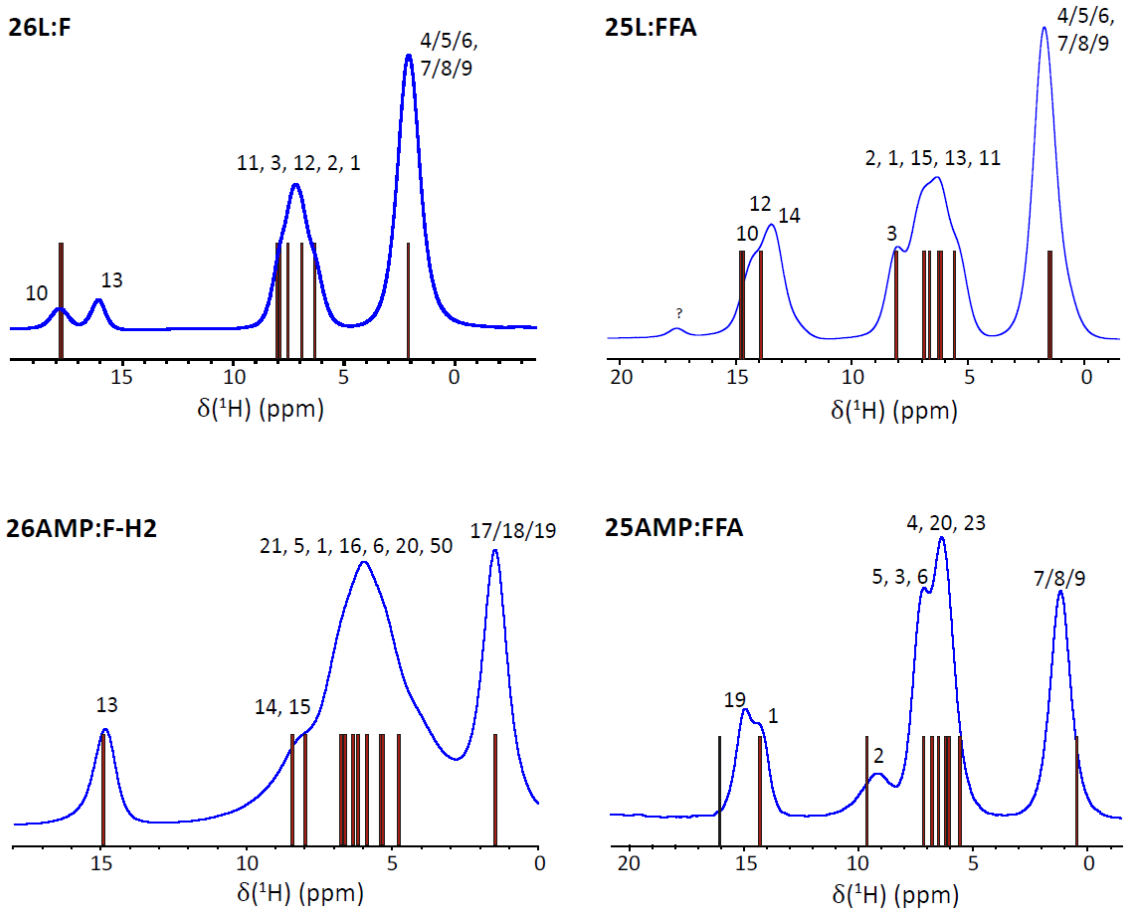

Figure 3: ^{1}H (600 MHz) one-pulse MAS (60 kHz) NMR spectra of 26L:F (top left), 25L:FFA (top right), 26AMP:F-H2 (bottom left) and 25AMP:FFA (bottom right) with stick spectra corresponding to GIPAW calculated chemical shifts for the geometry optimised crystal structures. The assignments to each proton are given (see Figure 1). For 25L:FFA (top right), a low intensity peak is observed between 17 and 18 ppm (denoted by ?); this is believed to correspond to a minority phase (note that this is largely obscured in the 1D ^{1}H-^{13}C CPMAS spectrum, presented below, due to both resonance overlap and the reduced signal to noise ratio).

As has been reported previously,[15] in 26L:F (Fig. 3), H13 is observed at a lower ppm value experimentally compared with GIPAW calculation and can be assigned to the peak at 15.8 ppm (rather than 17.7 ppm as calculated). The other high-ppm ^{1}H resonance, corresponding to the NH^{+}, has the same calculated chemical shift and is indeed seen experimentally at 17.7 ppm. The OH protons of FA, 25AMP:FFA and 25L:FFA also showed the largest discrepancy between experiment and calculation of the chemical shift. In the latter case, the experimental chemical shifts for the two OH protons in the system lie at δ_{iso}^{exp} = 13.4 ppm, at a lower ppm value than for the NH^{+} proton, despite both being calculated at a higher chemical shift than this NH^{+} environment. As in 26L:F, the NH^{+} in 26AMP:F-H2, 25AMP:FFA and 25L:FFA is at a similarly high chemical shift to the OH resonances but in each case shows good agreement with the GIPAW calculated chemical shift (Table 4). This suggests that the OH···O discrepancy is not simply explained by the known temperature dependence of hydrogen-bonded chemical shifts, [52-59] as this would also be expected to effect the $NH^{+}\cdots^{-}O$ proton.

The level of discrepancy between experiment and GIPAW calculation seen for each system is relatively consistent, with $\Delta\delta^{exp-calc}$ ranging from −1.9 to −1.2 ppm in 26L:F and FA, respectively. The

lowest magnitude $\Delta\delta^{exp\text{-}calc}$ of –1.2 ppm is for fumaric acid, where there is a neutral carboxylic acid/carboxylic acid hydrogen bond.

Table 4: GIPAW calculated and experimental MAS NMR ^{1}H chemical shifts (in ppm) for the OH and NH moieties in 26L:F, 25L:FFA, 25AMP:FFA, 26AMP:F-H2 and FA.

System	OH				NH			
	Atom	δ^{exp}	δ^{calc}	$\Delta\delta^{exp\text{-}calc}$	Atom	δ^{exp}	δ^{calc}	$\Delta\delta^{exp\text{-}calc}$
26L:F	H13	15.8	17.7	–1.9	H10	17.7	17.7	0.0
25L:FFA	H12/14	13.4/13.4	14.7/14.8	–1.3/–1.4	H10	14.3	13.9	0.4
25AMP:FFA	H19	14.7	16.0	–1.3	H1	14.0	14.2	–0.2
26AMP:F-H2	-	-	-	-	H13	14.9	14.8	0.1
FA		12.9[51]	14.1	–1.2	-	-	-	-

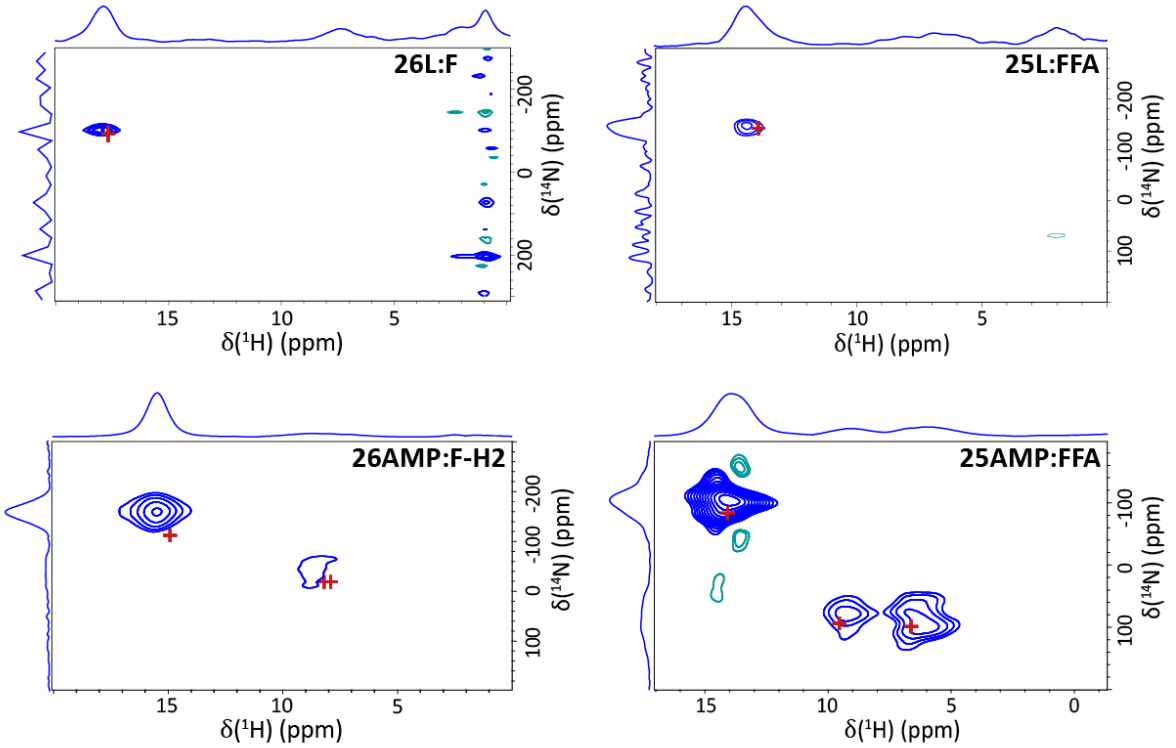

Figure 4: ^{14}N-^{1}H HMQC MAS (60 kHz) NMR spectra of 26L:F(top left), 25L:FFA (top right), 26AMP:F-H2 (bottom left) and 25AMP:FFA (bottom right) recorded with 8 rotor periods of R^3 recoupling (τ_{RCPL} = 133.6 μs). Spectra were recorded at ν_0 (^{1}H) 600 MHz with the exception of 26AMP:F-H2, recorded at ν_0 (^{1}H) = 700 MHz. Red crosses correspond to the GIPAW calculated shifts of the expected NH correlations (SI, Tables S1 to S5).

^{13}C environment

Fig. 5 shows ^{1}H-^{13}C CP MAS spectra for the four systems, with stick spectra corresponding to GIPAW calculated chemical shifts for the geometry optimised crystal structures. Assignments were made with the aid of the DFT calculations (SI, Tables S2-5).

In 26AMP:F-H2, C9 is calculated at 151.3 ppm but is instead observed experimentally at 155.5 ppm. 25AMP:FFA shows an even greater discrepancy with the calculated chemical shift for C1 5.9 ppm lower than the experimental value of 153.8 ppm. By comparison, the quaternary carbons that sit at the analogous position in both 25L:FFA and 26L:F, directly bound to the pyridinium nitrogen, show excellent agreement between experiment and calculation with the largest discrepancy 0.2 ppm (Table 5). As these are substituted with a methyl group rather than an amino group, the combination of amino and pyridinium interactions is thus correlated with the larger discrepancy between experiment and GIPAW calculation. No change in the ^{13}C chemical shift was observed when recorded at a ^{1}H Larmor frequency of 500 and 600 MHz (SI, Fig. S3), ruling out a shift of the ^{13}C chemical shift due to enhanced second-order quadrupolar effects from the two adjacent ^{14}N atoms. There is a known deviation from negative one in the gradient of a plot of experimental chemical shift against calculated chemical shielding, but this would be expected to affect the carboxyl and methyl carbons more significantly as they are further towards the edges of the chemical shift range. It is also of note that this would cause high-ppm ^{13}C environments to be calculated at a higher chemical shift than they are observed experimentally rather than lower, as seen for the amino substituted quaternary carbons discussed here.

To our knowledge, there are very few examples in the literature of such large discrepancies for ^{13}C: one example is that in 2006, Harris reported for the quaternary C5 site (fused between two 6-membered ring with one C=C and two C-C bonds) in testosterone GIPAW calculation at 182.6 and 182.7 compared to 170.6 and 172.0 ppm experimentally for the two distinct molecules in the asymmetric unit cell.[60]

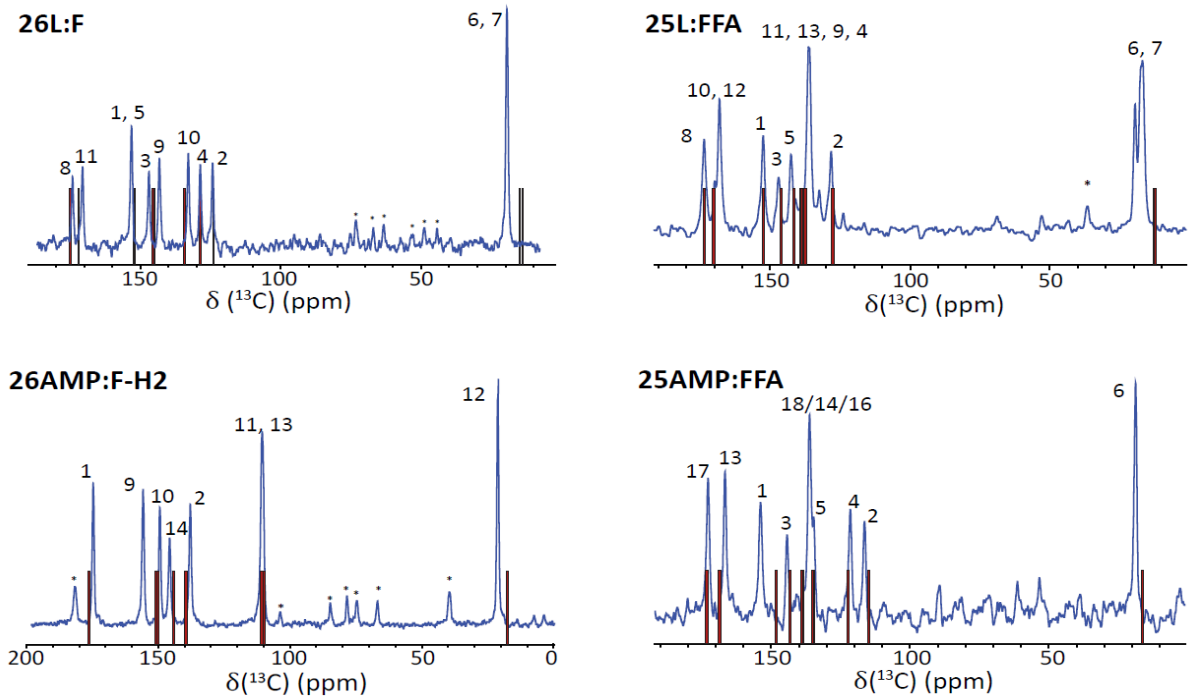

Figure 5: ^{1}H-^{13}C CP-MAS (12.5 kHz) spectra of 26L:F(top left), 25L:FFA (top right), 26AMP:F-H2 (bottom left) and 25AMP:FFA (bottom right), with stick spectra corresponding to GIPAW calculated chemical shifts. The assignments to each carbon are given (see Figure 1). Spectra were recorded at a ^{1}H Larmor frequency of 500 MHz (top) and 600 MHz (bottom).

Table 5: GIPAW calculated and experimental MAS NMR ^{13}C chemical shifts (in ppm) for the quaternary carbons at the 2-position on the pyridinium ring in 26L:F, 25L:FFA, 25AMP:FFA and 26AMP:F-H2.

System	^{13}C			
	Atom	δ^{exp}	δ^{calc}	$\Delta\delta^{exp-calc}$
26L:F	C1/5	152.6/152.6	152.4/152.6	0.2/0.0
25L:FFA	C1	152.4	152.5	0.1
25AMP:FFA	C9	153.8	147.9	5.9
26AMP:F-H2	C1	155.5	151.3	4.2

Conclusions

An NMR crystallography study has been presented that reports ^{1}H, ^{13}C chemical shifts and ^{14}N shifts for four differently substituted pyridine molecules and fumaric acid that occur as two salts and two cocrystals of a salt in the solid state. The focus of this paper is on two chemical environments for which a greater discrepancy is observed between experiment and GIPAW calculated chemical shifts that goes beyond the typically encountered maximum of 1% of the chemical shift range. These are the ^{1}H in an OH···O hydrogen bond (which is observed 1.2-1.9 ppm below its calculated position) and a quaternary ^{13}C sitting covalently bound to both a pyridinium nitrogen and an amino nitrogen (which is observed 4.2-5.9 ppm above its calculated position). These discrepancies between experiment and GIPAW calculation stand out because of the great success of such GIPAW calculations in reproducing experimental chemical shifts.

For the ^{1}H chemical shifts of the hydrogen-bonded fumaric acid protons, it would be interesting to investigate the temperature dependence[52-59] to see if there are marked differences for the fumaric acid OH ^{1}H resonances as compared to the NH^{+} ^{1}H resonances. In this context, there is also work that combines molecular dynamics with GIPAW simulation.[61-65] Note, however, that it is curious that this study has shown excellent agreement between experiment and GIPAW calculation for the NH^{+} ^{1}H resonances even though the GIPAW calculation corresponds to 0 K. In addition, it would be interesting to investigate whether these discrepancies change if alternative calculation approaches are employed, such as the use of a hybrid DFT functional, e.g., PBE0 or the combination of a GIPAW calculation with a calculation on an isolated molecule at a higher level of theory, as described by Beran and co-workers.[66-68]

Acknowledgments

Emily Corlett thanks EPSRC, AstraZeneca and Syngenta for a PhD studentship through the EPSRC Centre for Doctoral Training in Molecular Analytical Science, grant number EP/L015307/1. The European Research Council (ERC Starting Grant 639907 awarded to Jozef Lewandowski) and the University of Warwick funded the 700 MHz Bruker Avance III spectrometer used for a ^{14}N-^{1}H

experiment. Helpful discussions with Paul Hodgkinson and Chris Pickard are acknowledged. The calculated and experimental data for this study are provided as a supporting data set from WRAP, the Warwick Research Archive Portal at http://wrap.warwick.ac.uk/***.

Supporting Information

Tables of experimental and GIPAW calculated ^{1}H, ^{13}C chemical shifts and ^{14}N shifts; experimental and simulated PXRD patterns; comparison of ^{13}C CP MAS spectra recorded at two different magnetic fields (pdf).

References

1. C. J. Pickard and F. Mauri, *Physical Review B*, 2001, **63**, 245101.
2. S. E. Ashbrook and D. McKay, *Chem. Commun.*, 2016, **52**, 7186-7204.
3. B. Elena, G. Pintacuda, N. Mifsud and L. Emsley, *J. Am. Chem. Soc.*, 2006, **128**, 9555-9560.
4. R. K. Harris, *Solid State Sci.*, 2004, **6**, 1025-1037.
5. C. Bonhomme, C. Gervais, F. Babonneau, C. Coelho, F. Pourpoint, T. Azais, S. Ashbrook, J. Griffin, J. Yates, F. Mauri and C. Pickard, *Chem. Rev.*, 2012, **112**, 5733-5779.
6. T. Charpentier, *Solid State Nucl. Magn. Reson.*, 2011, **40**, 1-20.
7. D. L. Bryce, *Iucrj*, 2017, **4**, 350-359.
8. M. Chierotti and R. Gobetto, *Crystengcomm*, 2013, **15**, 8599-8612.
9. P. C. Vioglio, M. R. Chierotti and R. Gobetto, *Advanced Drug Delivery Reviews*, 2017, **117**, 86-110.
10. D. Dudenko, J. Yates, K. Harris and S. Brown, *Crystengcomm*, 2013, **15**, 8797-8807.
11. C. M. Gowda, F. Vasconcelos, E. Schwartz, E. R. H. van Eck, M. Marsman, J. J. L. M. Cornelissen, A. E. Rowan, G. A. de Wijs and A. P. M. Kentgens, *Physical Chemistry Chemical Physics*, 2011, **13**, 13082-13095.
12. P. Paluch, T. Pawlak, M. Oszajca, W. Lasocha and M. Potrzebowski, *Solid State Nuclear Magnetic Resonance*, 2015, **65**, 2-11.
13. G. Reddy, D. Cook, D. Iuga, R. Walton, A. Marsh and S. Brown, *Solid State Nuclear Magnetic Resonance*, 2015, **65**, 41-48.
14. J. Yates, T. Pham, C. Pickard, F. Mauri, A. Amado, A. Gil and S. Brown, *Journal of the American Chemical Society*, 2005, **127**, 10216-10220.
15. E. K. Corlett, H. Blade, L. P. Hughes, P. J. Sidebottom, D. Walker, R. I. Walton and S. P. Brown, *Crystengcomm*, 2019, **21**, 3502-3516.
16. R. K. Harris, P. Y. Ghi, H. Puschmann, D. C. Apperley, U. J. Griesser, R. B. Hammond, C. Y. Ma, K. J. Roberts, G. J. Pearce, J. R. Yates and C. J. Pickard, *Org. Process. Res. Dev.*, 2005, **9**, 902-910.
17. J. R. Yates, S. E. Dobbins, C. J. Pickard, F. Mauri, P. Y. Ghi and R. K. Harris, *Phys. Chem. Chem. Phys.*, 2005, **7**, 1402-1407.
18. A. L. Webber, L. Emsley, R. M. Claramunt and S. P. Brown, *J. Phys. Chem. A*, 2010, **114**, 10435-10442.
19. D. V. Dudenko, P. A. Williams, C. E. Hughes, O. N. Antzutkin, S. P. Velaga, S. P. Brown and K. D. M. Harris, *J. Phys. Chem. C*, 2013, **117**, 12258-12265.
20. A. C. Poppler, E. K. Corlett, H. Pearce, M. P. Seymour, M. Reid, M. G. Montgomery and S. P. Brown, *Acta Crystallogr., Sect. C: Cryst. Struct. Commun.*, 2017, **73**, 149-156.
21. E. A. Engel, A. Anelli, A. Hofstetter, F. Paruzzo, L. Emsley and M. Ceriotti, *Physical Chemistry Chemical Physics*, 2019, **21**, 23385-23400.
22. X. Li, L. Tapmeyer, M. Bolte and J. van de Streek, *Chemphyschem*, 2016, **17**, 2496-2502.

23. O. Almarsson and M. Zaworotko, *Chemical Communications*, 2004, 1889-1896.
24. C. Aakeroy and D. Salmon, *Crystengcomm*, 2005, **7**, 439-448.
25. P. Vishweshwar, J. McMahon, J. Bis and M. Zaworotko, *Journal of Pharmaceutical Sciences*, 2006, **95**, 499-516.
26. A. Trask, *Molecular Pharmaceutics*, 2007, **4**, 301-309.
27. S. M. Berge, L. D. Bighley and D. C. Monkhouse, *Journal of Pharmaceutical Sciences*, 1977, **66**, 1-19.
28. S. L. Childs, G. P. Stahly and A. Park, *Molecular Pharmaceutics*, 2007, **4**, 323-338.
29. C. R. Groom, I. J. Bruno, M. P. Lightfoot and S. C. Ward, *Acta Crystallogr., Sect. B: Struct. Sci.*, 2016, **72**, 171-179.
30. Y. Pan, Z. Jin, C. Sun and C. Jiang, *Chemistry Letters*, 2001, **30**, 1008-1009.
31. D. A. Haynes, W. Jones and W. D. S. Motherwell, *Crystengcomm*, 2006, **8**, 830-840.
32. M. Hemamalini and H. Fun, *Acta Crystallographica Section E-Structure Reports Online*, 2010, **66**, O2093-U1847.
33. S. Selyani and M. Dincer, *Molecular Crystals and Liquid Crystals*, 2018, **666**, 65-78.
34. C. J. Brown, *Acta. Cryst.*, 1966, 1-5.
35. S. J. Clark, M. D. Segall, C. J. Pickard, P. J. Hasnip, M. J. Probert, K. Refson and M. C. Payne, *Z. Kristallogr.*, 2005, **220**, 567-570.
36. J. P. Perdew, K. Burke and M. Ernzerhof, *Phys. Rev. Lett.*, 1996, **77**, 3865-3868.
37. G. N. M. Reddy, D. S. Cook, D. Iuga, R. I. Walton, A. Marsh and S. P. Brown, *Solid State Nucl. Magn. Reson.*, 2015, **65**, 41-48.
38. R. K. Harris, P. Hodgkinson, C. J. Pickard, J. R. Yates and V. Zorin, *Magn. Reson. Chem.*, 2007, **45**, S174-S186.
39. S. Cavadini, S. Antonijevic, A. Lupulescu and G. Bodenhausen, *J. Magn. Reson.*, 2006, **182**, 168-172.
40. S. Cavadini, *Prog. Nucl. Magn. Reson. Spectrosc.*, 2010, **56**, 46-77.
41. A. S. Tatton, J. P. Bradley, D. Iuga and S. P. Brown, *Z. Phys. Chem.*, 2012, **226**, 1187-1203.
42. Z. H. Gan, J. P. Amoureux and J. Trebosc, *Chem. Phys. Lett.*, 2007, **435**, 163-169.
43. M. H. Levitt, T. G. Oas and R. G. Griffin, *Isr. J. Chem.*, 1988, **28**, 271-282.
44. T. G. Oas, R. G. Griffin and M. H. Levitt, *J. Chem. Phys.*, 1988, **89**, 692-695.
45. D. Marion, M. Ikura, R. Tschudin and A. Bax, *J. Magn. Reson.*, 1989, **85**, 393-399.
46. B. M. Fung, A. K. Khitrin and K. Ermolaev, *J. Magn. Reson.*, 2000, **142**, 97-101.
47. G. Metz, X. L. Wu and S. O. Smith, *J. Magn. Reson., Ser A*, 1994, **110**, 219-227.
48. S. Hayashi and K. Hayamizu, *Bull. Chem. Soc. Jpn.*, 1991, **64**, 685-687.
49. C. R. Morcombe and K. W. Zilm, *J. Magn. Reson.*, 2003, **162**, 479-486.
50. S. Hayashi and K. Hayamizu, *Bull. Chem. Soc. Jpn.*, 1991, **64**, 688-690.
51. R. K. Harris, P. Jackson, L. H. Merwin, B. J. Say and G. Hagele, *J. Chem. Soc.*, 1988, **84**, 3649-3672.
52. S. P. Brown, I. Schnell, J. D. Brand, K. Mullen and H. W. Spiess, *PCCP*, 2000, **2**, 1735-1745.
53. N. Muller and R. C. Reiter, *J. Chem. Phys.*, 1965, **42**, 3265-3269.
54. J. T. Arnold and M. E. Packard, *J. Chem. Phys.*, 1951, **19**, 1608-1609.
55. U. Liddel and N. F. Ramsey, *J. Chem. Phys.*, 1951, **19**, 1608.
56. K. Modig and B. Halle, *JACS*, 2002, **124**, 12031-12041.
57. Y. Li, Y. M. Jia, Z. W. Wang, X. H. Li, W. Feng, P. C. Deng and L. H. Yuan, *Rsc Advances*, 2014, **4**, 29702-29714.
58. A. L. Webber, B. Elena, J. M. Griffin, J. R. Yates, T. N. Pham, F. Mauri, C. J. Pickard, A. M. Gil, R. Stein, A. Lesage, L. Emsley and S. P. Brown, *Physical Chemistry Chemical Physics*, 2010, **12**, 6970-6983.
59. J. N. Dumez and C. J. Pickard, *J. Chem. Phys.*, 2009, **130**, 104701.
60. R. K. Harris, S. A. Joyce, C. J. Pickard, S. Cadars and L. Emsley, *Physical Chemistry Chemical Physics*, 2006, **8**, 137-143.

61. M. Dracinsky and P. Hodgkinson, *Chem. Eur.*, 2014, **20**, 2201-2207.
62. M. Dracinsky and P. Hodgkinson, *Crystengcomm*, 2013, **15**, 8705-8712.
63. M. Dracinsky, L. Cechova, P. Hodgkinson, E. Prochazkova and Z. Janeba, *Chem. Comm.*, 2015, **51**, 13986-13989.
64. M. Dracinsky, P. Bour and P. Hodgkinson, *Journal of Chemical Theory and Computation*, 2016, **12**, 968-973.
65. I. De Gortari, G. Portella, X. Salvatella, V. S. Bajaj, P. C. A. van der Wel, J. R. Yates, M. D. Segall, C. J. Pickard, M. C. Payne and M. Vendruscolo, *J. Am. Chem. Soc.*, 2010, **132**, 5993-6000.
66. J. D. Hartman, R. A. Kudla, G. M. Day, L. J. Mueller and G. J. O. Beran, *Phys. Chem. Chem. Phys.*, 2016, **18**, 21686-21709.
67. M. Dracinsky, P. Unzueta and G. Beran, *Physical Chemistry Chemical Physics*, 2019, **21**, 14992-15000.
68. J. D. Hartman, S. Monaco, B. Schatschneider and G. J. O. Beran, *Journal of Chemical Physics*, 2015, **143**.

TOC graphic